Turkish Journal of Electrical Engineering & Computer Sciences

http://journals.tubitak.gov.tr/elektrik/

Research Article

Turk J Elec Eng & Comp Sci
(2016) 24: 4042 – 4062

doi:10.3906/elk-1410-107

Fuzzy based design of digital IIR filter using ETLBO

Damanpreet SINGH[1,*], **Jaspreet Singh DHILLON**[2]

[1]Department of Computer Science and Engineering, Sant Longowal Institute of Engineering and Technology, Longowal, Punjab, India

[2]Department of Electrical & Instrumentation Engineering, Sant Longowal Institute of Engineering and Technology, Longowal, Punjab, India

Received: 19.10.2014 • **Accepted/Published Online:** 05.07.2015 • **Final Version:** 20.06.2016

Abstract: In this paper, a population-based robust enhanced teaching–learning-based optimization (ETLBO) algorithm with reduced computational effort and high consistency is applied to design stable digital infinite-impulse response (IIR) filters in a multiobjective framework. Furthermore, a decision-making methodology based on fuzzy set theory is applied to handle nonlinear and multimodal design problems of the IIR digital filter. The original teaching–learning-based optimization (TLBO) algorithm has been remodeled by merging the concepts of opposition-based learning and migration for the selection of good candidates and to maintain diversity, respectively. A multiobjective IIR digital filter design problem takes into consideration magnitude and phase response of the filter simultaneously, while satisfying stability constraints on the coefficients of the filter. The order of the filter is controlled by a control gene whose value is also along with filter coefficients, to obtain the optimum order of the designed IIR filter. Results illustrate that ETLBO is more capable and efficient in comparison to other optimization methods for the design of all types of filter, i.e. high-pass, low-pass, band-stop, and band-pass IIR digital filters.

Key words: Digital infinite impulse response filters, teaching–learning-based optimization, magnitude response, phase response, filter order

1. Introduction

The digital filter is a basic component of all signal processing and communication systems. In digital signal processing, the role of a filter is to extract the informative component of the signal, such as the segments lying in between a particular frequency range, or to remove undesirable parts of the signal, such as random noise. Digital filters are widely categorized as infinite impulse response (IIR) and finite impulse response (FIR) filters. Digital IIR filters are mostly preferred in comparison to FIR filters, as IIR digital filters achieve high selectivity with a significantly lower filter order [1].

In recent decades, the design of digital IIR filters has attracted considerable attention from researchers. There are no conventional design methods for designing optimal digital filters [2]. The performance of the IIR filter designed with transformation techniques is not up to the mark and involves too much prior knowledge. The main problems in IIR filter design are [3]: 1) the nonlinear and multimodal error surface of the filter; 2) the filter becoming unstable; 3) achieving linear-phase response; 4) the magnitude response and phase linearity are conflicting in nature when considered simultaneously; 5) locating the lowest filter order; 6) satisfying the pass-band and stop-band ripple tolerances. Filter stability can be controlled by constraining the variable values

*Correspondence: damanpreetsingh@sliet.ac.in

in the required range so that all the poles are inside the unit circle in the z-plane. The relevance of phase approximation error is much greater than that of the group delay error in digital IIR filters, because, compared to group delay error, magnitude and phase errors are used to control the amplitude of undesired echoes in the output of the filter [4]; in addition, various frequency components of the signal are altered due to nonlinear phase response.

The intent of IIR filter design problem is to optimize the filter order, magnitude response, and phase response so that the designed filter meets the desired design specifications. Digital filter design primarily consists of the following steps [3]: 1) conversion of the desired design constraints into precise specifications or criteria; 2) approximation of the filter coefficients of the IIR filter such that the magnitude response, phase response error, and order are minimized, by employing some error criterion.

The multimodal and nonlinear error surface of digital IIR filters may lead to the trapping of conventional design algorithms at a local minimum [1,5]. To find a solution to this problem and to reach the global optimum, the various global optimization-based algorithms for designing IIR digital filters proposed in the literature include genetic algorithms (GAs) [6–8], simulated annealing [9], ant colony optimization [10], tabu search [11], immune algorithms [12], particle swarm optimization [13], seeker-optimization algorithms [14], real structured genetic algorithms [15], multiobjective optimization evolutionary algorithms [16], two-stage ensemble evolutionary algorithms [17], and gravitational search algorithms [18].

The ability to find the optimum solution in almost all evolutionary and swarm intelligence-based methods is dependent upon the tuning of controlling parameters such as the size of the population, number of iterations, group size, etc. For example, a genetic algorithm requires determining the optimum value of algorithm-specific parameters such as mutation operator, crossover operators, etc. An artificial bee colony requires researchers to estimate the number of bees engaged, scout bees, onlooker bees, and limits. Particle swarm optimization requires researchers to determine swarm size, maximum velocity, and acceleration constants. Recently, Rao et al. [19,20] proposed a teaching–learning-based optimization (TLBO) algorithm influenced by the social phenomenon of teaching–learning. The implementation of TLBO does not require specific controlling parameters, thus resulting in an increase of the robustness of the algorithm. The main controlling parameter in TLBO is population size. Hence, TLBO can be treated as a parameterless algorithm. The performance of the TLBO algorithm for various constrained benchmark problems was investigated by Rao and Patel [21] for different sizes of populations, elite sizes, and number of iterations to study their effect on the exploration and exploitation capability of the TLBO.

In IIR digital filter design, simultaneous consideration of magnitude response, phase response, filter stability, and filter order with less computation burden is a challenging task. Recently, researchers have designed an IIR filter that meets all the above requirements with the hierarchal genetic algorithm (HGA) [6], cooperative coevolutionary genetic algorithm (CCGA) [8], and a new local search operator enhanced multiobjective evolutionary algorithm (LS-MOEA) [16]. The aim of this paper is to further satisfy the solution methodology of multiobjective IIR filter design by considering magnitude response, phase response, filter stability, and order of the filter simultaneously by applying an efficient heuristic optimization algorithm, namely ETLBO. The exploration and exploitation capabilities of the original TLBO are improved by initializing with good candidates by employing the theory of opposition-based learning, and maintaining diversity by applying migration. Furthermore, fuzzy set theory has been employed in finding a solution for decision-making problems involving the numerous and imprecise nature of objectives and selection criteria for the best compromise solution. The effectiveness of the proposed method is tested for high-pass (HP), low-pass (LP), band-stop (BS), and band-pass (BP) IIR digital filters and compared to the previous research reported in [6,8,16].

The paper is structured as follows. The digital IIR filter design is formulated in Section 2. Section 3 describes the implementation of the ETLBO algorithm for the design of optimal digital IIR filters. The performance of ETLBO is evaluated and compared with the design obtained by other researchers [6,8,16] in Section 4. Finally, Section 5 concludes the outcomes of the work.

2. Description of the problem

The stable IIR filter becomes unstable if an appropriate realization structure is not chosen. In this paper, the cascade form of implementation for realization of the IIR filter is considered because the locations of the poles and zeros will not change when coefficients are quantized. The fundamental cascaded structure regardless of the filter type is [6]:

$$H(z) = x_1 \times \left(\left(\prod_{k=1}^{u} \frac{1 + x_{2k} z^{-1}}{1 + x_{2k+1} z^{-1}} \right) \times \left(\prod_{i=1}^{v} \frac{1 + x_{4i+2u-2} z^{-1} + x_{4i+2u-1} z^{-2}}{1 + x_{4i+2u} z^{-1} + x_{4i+2u+1} z^{-2}} \right) \right). \tag{1}$$

$X = [x_1, x_2, ..., x_{2u+4v+1}]^T_{S\times 1}$ is a vector decision variable of dimension $S \times 1$, with $S = 2u + 4v + 1$. x_1 represents the gain and $[x_2, x_3, ... x_{2u+4v+1}]$ denotes the filter coefficients of the first- and second-order sections.

2.1. Magnitude response error

The magnitude response conditions considered for the design of a digital IIR filter are as follows:

- The pass-band ripples should be less than or equal to δ_P.
- The stop-band ripples should not exceed δ_s.

The pass-band and stop-band edge discrete frequencies for digital IIR filters are represented by ω_j and ω_k, respectively. The aim is to minimize the magnitude response of the defined frequency band in which either frequency is allowed to pass or restrict.

The fuzzy set theory is employed for the purpose of decision-making involving multiple objectives, namely magnitude response in the pass-band and stop-band. Equations called membership functions are used to define fuzzy sets, which denote the target of each objective function. The degree of accomplishment of the original objective function is represented by the membership function, whose value ranges between 0 and 1. Membership function value 1 gives a completely satisfactory objective, and 0 value of membership function gives an unsatisfactory objective. The membership function μ_i is determined considering the lower and upper values of the individual objective function, along with the pace of enhancement of membership satisfaction [22]. The membership function for the pass band magnitude response, μ^p_{1j} for the jth frequency sampling point, is realized by the trapezoidal membership function and membership function for the stop-band magnitude response; μ^s_{2k} for the kth frequency sampling point is realized by the monotonic decreasing function. Graphic representations are given in Figure 1, and membership functions are defined mathematically as follows:

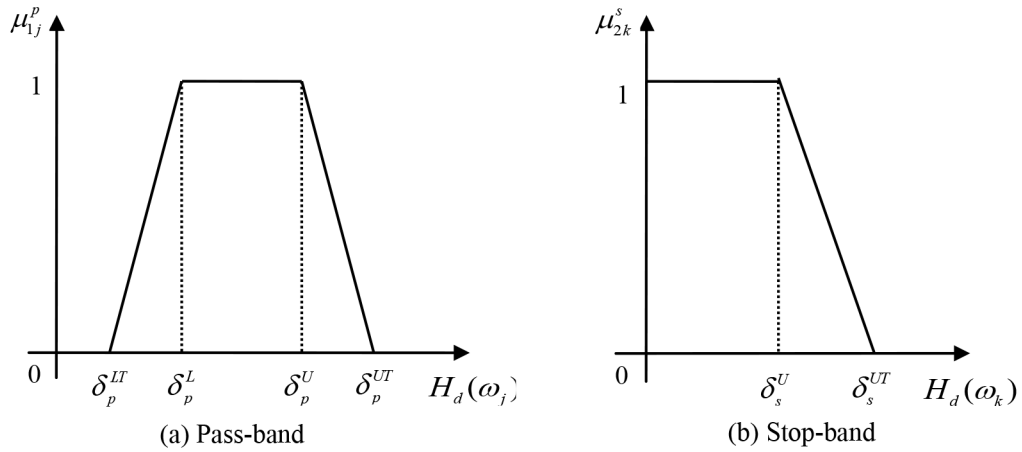

Figure 1. Membership function for magnitude performance of pass-band and stop-band.

$$\mu_{1j}^{p} = \begin{cases} 0; H_d(\omega_j) \le \delta_p^{LT} \\ \frac{H_d(\omega_j)-\delta_p^{LT}}{\delta_p^{L}-\delta_p^{LT}}; \delta_p^{LT} \le H_d(\omega_j) \le \delta_p^{L} \\ 1; \delta_p^{L} \le H_d(\omega_j) \le \delta_p^{U} \\ \frac{\delta_p^{UT}-H_d(\omega_j)}{\delta_p^{UT}-\delta_p^{U}}; \delta_p^{U} \le H_d(\omega_j) \le \delta_p^{UT} \\ 0; H_d(\omega_j) \ge \delta_p^{UT} \end{cases} \quad (j = 1, 2..., A_n), \tag{2}$$

$$\mu_{2k}^{s} = \begin{cases} 1; H_d(\omega_k) \le \delta_s^{U} \\ \frac{\delta_s^{UT}-H_d(\omega_k)}{\delta_s^{UT}-\delta_s^{U}}; \delta_s^{U} \le H_d(\omega_k) \le \delta_s^{UT} \\ 0; H_d(\omega_k) \ge \delta_s^{UT} \end{cases} \quad (k = 1, 2..., B_n), \tag{3}$$

where A_n and B_n are the sampling frequency points in the pass-band and stop-band, respectively.

$H_d(\omega_j)$ and $H_d(\omega_k)$ are the magnitude response of the designed digital IIR filter in the pass-band and stop-band, respectively.

δ_p^{L} and δ_p^{U} are lower and upper allowable range values of ripples in the pass-band.

δ_p^{LT} and δ_p^{UT} are lower and upper range transition values of ripples in the pass-band, giving the degree of acceptance of magnitude error.

δ_s^{U} is the upper allowable range value of ripples in the stop-band.

δ_s^{UT} is the upper range transition values of ripples in the stop-band, giving the degree of acceptance of magnitude error.

The objective functions μ_1 and μ_2 for the pass-band and stop-band magnitude performance can be formulated by considering the cumulative effect of the pass-band and stop-band of the frequency band:

$$\begin{array}{l} \mu_1 = \frac{1}{A_n} \sum_{j=1}^{A_n} \mu_{1j}^p \\ \mu_2 = \frac{1}{B_n} \sum_{k=1}^{B_n} \mu_{1k}^s \end{array} . \tag{4}$$

The overall objective function O_1 for magnitude response error is redefined by considering the intersection of the membership function of μ_1 and μ_2 to obtain the greater satisfaction level of the objective function, and it is stated below:

$$O_1 = Min\left\{\mu_1, \mu_2\right\}. \tag{5}$$

In the design of the IIR digital filter, a fixed grid approach is used [23]. The frequency range from 0 to π is divided into a fixed number of evenly divided sample points. The best fitness function value is achieved when the magnitude response of the designed digital IIR filter lies within the prescribed tolerance range in the pass-band and stop-band.

2.2. Phase response error

The linear phase response is optimized for both the pass-band and the transition band [9,10], because sometimes nonlinearity in the phase response of the transition band may cause distortion. The phase response of the IIR filter is defined as:

$$phase = \arg\left|H(e^{j\omega})\right|. \tag{6}$$

The phase response is calculated at different frequency sampling points $\{\alpha_1, \alpha_2, ..., \alpha_l\}$. The first-order difference in the phase response can be calculated as:

$$\beta(\omega) = \arg\left|H(e^{j\omega})\right|, \tag{7}$$

$$f_2 = \Delta phase = \left\{\Delta\alpha_1, \Delta\alpha_2, ..., \Delta\alpha_{l-1}\right\}, \tag{8}$$

where $\Delta\alpha_l = \alpha_{l+1} - \alpha_l$; l is the total number of sampling points in the pass-band and transition band. The phase response is linear if all the elements of $\Delta\, phase$ have the same value. The second objective function in terms of linear phase response error is represented as the variance of phase differences.

$$\begin{array}{l} O_2 = \frac{1}{1+var\{\Delta\alpha_l\}} \\ \text{where } \alpha_l \in \text{ pass-band } \cup \text{transition band} \end{array} \tag{9}$$

2.3. Multiobjective IIR filter problem formulation

The design of an IIR filter involves obtaining the optimum structure of the filter having optimal order, minimum tmagnitude, and minimum phase response error. Mathematically, the multiobjective optimization problem of digital IIR filter design is stated below:

$$\text{Maximize membership function of magnitude error performance } O_1(X); \tag{10a}$$

$$\text{Maximize fitness function of phase response } O_2(X); \tag{10b}$$

Subject to: stability constraints [24]:

$$1 + x_{2k+1} \geq 0 (k = 1, 2, ..., u), \tag{10c}$$

$$1 - x_{2k+1} \geq 0 (k = 1, 2, ..., u), \tag{10d}$$

$$1 - x_{4i+2u+1} \geq 0 (i = 1, 2, ..., v), \tag{10e}$$

$$1 + x_{4i+2u} + x_{4i+2u+1} \geq 0 (i = 1, 2, ..., v), \tag{10f}$$

$$1 - x_{4i+2u} + x_{4i+2u+1} \geq 0 (i = 1, 2, ..., v), \tag{10g}$$

where $O_1(X)$, given by Eq. (5), is the membership function of the magnitude response error, and $O_2(X)$, given by Eq. (9), is the fitness function of the variance of phase difference. X is a vector decision variable of dimensions $S \times 1$ with $S = 2u + 4v + 1$.

The aim is to find the value of filter coefficients being decision variables, X, that optimizes all the objective functions simultaneously. The multiobjective constrained optimization problem of IIR digital filter design is converted into a scalar constrained optimization problem by the selection of min–max of the membership function as defined below [25]:

$$F(X) = Max \left[Min \left\{ O_i(X) (i = 1, 2) \right\} \right], \tag{11}$$

subject to fulfillment of the stability constraints given in Eqs. (10c) to (10g).

2.4. Order

The order of an IIR digital filter is defined as the largest number of previous input values or output values needed to calculate the current value of output. The higher the filter order, the greater the complexity will be. Mathematically, the order of the IIR filter is determined as follows:

$$Order = \sum_{j=1}^{u} p_j + 2 \sum_{k=1}^{v} q_k, \tag{12}$$

where p_j and q_k are the jth and kth control genes respectively for corresponding first-order and second-order blocks; u and v are the number of first- and second-order blocks, respectively. The maximum order of the filter is $u + 2v$.

The structure of the digital IIR filter is represented by the control gene (Figure 2). The coding method followed was that used in [6,8,16]. The control genes determine activation/deactivation of corresponding blocks of filter coefficients by setting 1/0, respectively. The value of binary bits used to generate control genes is evaluated based on the integer value of the variable $x_{2u+4v+2}$ of decision vector X. The integer value of variable $x_{2u+4v+2}$ is optimized along with the filter coefficients to obtain the optimum order of the designed IIR filter.

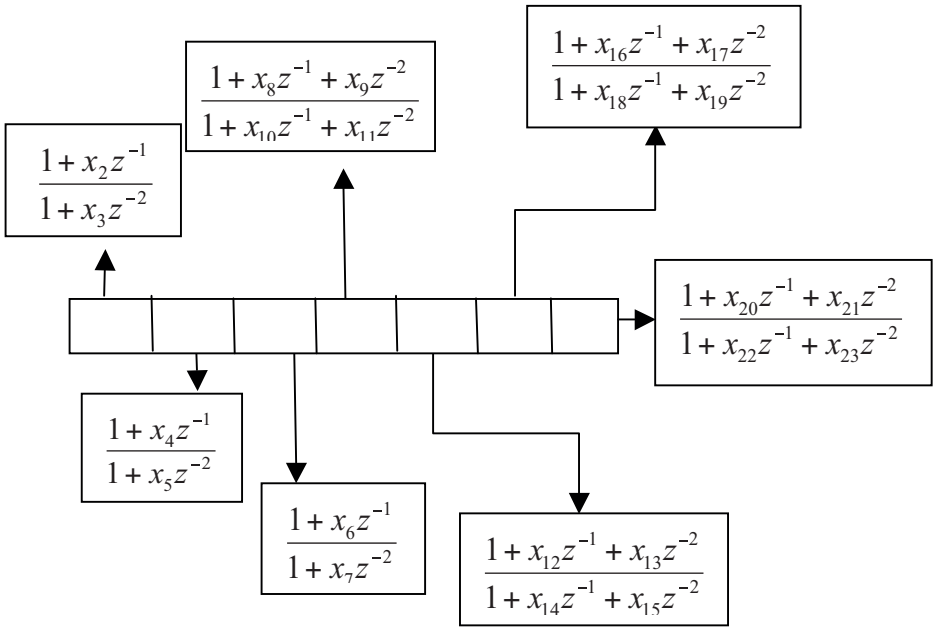

Figure 2. Activation/deactivation of filter coefficients with control gene.

$X = [x_1, x_2, ..., x_{2u+4v+1}, x_{2u+4v+2}]^T_{S\times 1}$ is the final decision variable where $S = 2u + 4v + 2$.

2.5. Constraint handling

The digital IIR filter design requires the satisfaction of stability constraints. The stability constraints on the coefficients of the digital IIR filter in Eq. (1) are obtained by using the Jury method [24].

The values of filter coefficients are updated with a random variation as given below in order to satisfy the stability constraints given by Eq. (10c) to Eq. (10g). Care is taken that the amount of variation is small enough that it should not change the characteristics of the population.

$$x_{2k+1} = \begin{cases} x_{2k+1}(1-r)^2; (1+x_{2k+1}) < 0 or (1-x_{2k+1}) < 0 \\ x_{2k+1};\ \text{Otherwise} \end{cases}, \tag{13a}$$

$$x_{4i+2u+1} = \begin{cases} x_{4i+2u+1}(1-r)^2; (1-x_{4i+2u+1}) < 0 \\ x_{4i+2u+1};\ \text{Otherwise} \end{cases}, \tag{13b}$$

$$x_{4i+2u} = \begin{cases} x_{4i+2u}(1-r)^2; (1+x_{4i+2u}+x_{4i+2u+1}) < 0 or (1-x_{4i+2u}+x_{4i+2u+1}) < 0 \\ x_{4i+2u};\ \text{Otherwise} \end{cases}, \tag{13c}$$

where r is a uniform random number whose value varies within [0, 1]. The square term ensures that the value of increment is small.

3. ETLBO algorithm

ETLBO inherits and works on a noble process, namely the concept of teaching–learning. It falls into the category of nature-inspired, population-based algorithms. In ETLBO, the population consists of the students in a class, and subjects offered to students represent different design variables. A set of good scores for the subject offered to students is initialized by applying opposition-based learning; further migration has been employed to maintain the diversity of the students. The candidate solution refers to the value of design variables, and the know-how of a particular student is analogous to the objective function [26].

A teacher is a role model and greatly influences the growth of society. ETLBO efficiently utilizes the knowledge base of a teacher to increase and improve the know-how of learners/students. The learners also further improve their knowledge base by interacting and sharing information with each other. The methodology of ETLBO consists of 2 main phases, the Teacher phase and the Learner phase.

3.1. Implementation of ETLBO

ETLBO is implemented by searching for the value of filter coefficients being decision variables, X, that optimizes all the objective functions. The stepwise procedure to implement the proposed algorithm is elaborated in the following subsections.

3.2. Class representation

Assume that NL is the number of students/learners in a class (population) and each learner has been assigned S subjects. The ith learner is represented by $X_i = [x_{i1}, x_{i2}, ...x_{iS}]$.

The decision variables of the digital IIR filter design problem are coefficients of the filter; hence, they are used to form the class. The set of filter coefficients (x_i) is represented as the subjects assigned to learners in a class. For a filter with S coefficients, the learner is represented by a vector of length S. Assuming there are NL learners in a class, the class is represented in the form of a matrix:

$$class = \begin{bmatrix} x_{11} & x_{12} & .. & .. & x_{1S} \\ x_{21} & x_{22} & .. & .. & x_{2S} \\ . & . & x_{ij} & .. & . \\ . & . & .. & .. & . \\ x_{NL1} & x_{NL2} & .. & .. & x_{NLS} \end{bmatrix}_{NL \times S},$$

where x_{ij} is the jth subject score of the ith learner.

3.3. Initialization of the class

Each learner of the class is initialized with the help of a random search for marks of all the subjects. The starting point is recorded by employing a global search, and then the starting point is further refined by giving small movements in the neighboring locality to find the best starting point. The variables are initialized using Eq. (14) to start the search process:

$$x_{ij}^t = x_j^{\min} + R()(x_j^{\max} - x_j^{\min})(i = 1, 2, ..., NL; j = 1, 2, ..., S), \tag{14}$$

where:

R is a uniform random generated number within {0, 1};

S is the number of subjects allotted to each learner;

NL is number of learners in a class;

t is the iteration counter;

$x_j^{\max}$ and $x_j^{\min}$ are the upper and lower range values of the jth decision variable (filter coefficient) of vector X.

3.4. Opposition-based learning

The convergence rate of ETLBO has been further enhanced with the help of opposition-based learning (OBL) [27]. The theory of opposition-based learning has already been applied to expedite the process of reinforcement learning and backpropagation learning in neural networks [28]. The concept behind opposition-based learning is to select a better current candidate solution by comparing the current population and its opposite population. Opposition-based learning is applied using Eq. (15) to record the alternative starting point, and the starting point x_{ij}^t is further explored using:

$$x_{i+NL,j}^t = x_j^{\max} - R()(x_j^{\max} - x_j^{\min})(i = 1, 2, ..., NL; j = 1, 2, ..., S). \tag{15}$$

Out of $2 \times NL$ learners, the best NL learners constitute a class to initiate the process. For the global search, the best learner is selected out of the class of learners.

Furthermore, opposition-based learning is also employed for generating new learners after completion of the learner phase, using Eq. (16):

$$x_{i+NL,j}^t = x_j^U + x_j^L - x_{ij}(i = 1, 2, ..., NL; j = 1, 2, ..., S), \tag{16}$$

where:

$$x_j^U = \max\{\, x_{ij}\,; \quad (i = 1,\ 2,\ ..., NL)\} \quad (j = 1,\ 2,\ ..., S),$$

$$x_j^L = \min\{\, x_{ij}\,; \quad (i = 1,\ 2,\ ..., NL)\} \quad (j = 1,\ 2,\ ..., S).$$

3.5. Function evaluation

The function f is evaluated from the maximum satisfaction level of all objective functions. The membership function of the ith learner of the class in the tth iteration used to solve the design of the IIR filter is given below:

$$f_i^t = \text{Maximize } \{F_i^t(x); (i = 1, 2..., NL)\}. \tag{17}$$

$F_i^t(X)$ is obtained using Eq. (11) for the ith learner of class in the tth iteration.

3.6. Teacher phase

Out of $2 \times NL$ learners generated in the initialization phase, the best NL learners are selected and evaluated based on the values of the fitness function. The best learner thus selected is designated as the teacher for the class. A teacher puts forth his/her best effort in order to increase/improve the mean score of all learners in each allotted subject towards its own mean score. Thus, the mean fitness of the class is increased by the teacher according to his/her own capability.

The best learner is selected from all the learners in a class based on the fitness function value calculated using Eq. (17) and acts as teacher xt_j^t for current iteration t. The mean (m_j) for S subjects allotted to the

students is evaluated, and a randomly weighted differential vector (D_j) from the current mean and various desired mean vectors [29] is calculated as given below:

$$m_j^t = \frac{1}{NL}\sum_{i=1}^{NL}(x_{i,j}^t)(j = 1, 2, ..., S), \tag{18}$$

$$D_j^t = R() \times (xt_j^t - (T_f \times m_j^t)(j = 1, 2, ..., S), \tag{19}$$

where:

m_j^t is the mean of the jth subject for all learners of a class;

xt_j^t is the score of the teacher of the jth subject;

T_f is the teaching factor;

R is a uniform generated random number within {0, 1}.

The convergence of ETLBO is facilitated by one important parameter, namely teaching factor (T_f). The value of T_f determines the volume of effect a teacher has on the output of a learner. High T_f leads the learners to drift away from good solutions, whereas too low a T_f restricts the learner's movement in a limited range and leads to slow convergence. In this paper, the value of T_f is selected as either 1 or 2 and is heuristically decided as follows:

$$T_f = ROUND(1.0 + R()). \tag{20}$$

The weighted differential vector (D_j) generated using Eq. (19) is added to the current score of learners in different subjects to generate new learners:

$$xnew_{ij}^t = x_{ij}^t + D_j^t(j = 1, 2, ..., S). \tag{21}$$

The newly generated learner with a better fitness value replaces the existing learner in the class.

3.7. Learner phase

The knowledge acquired by the learners from the teacher is further disseminated by learners among themselves by interacting on a regular basis through the sharing of notes, discussions, and presentations. The second phase of ETLBO emulates this sharing of knowledge by learners among themselves. Two target learners, namely i and k, are selected randomly such that $i \neq k$. After sharing/exchange of know-how, the resultant new learners are generated as follows:

$$xnew_{ij}^t = \begin{cases} x_{ij}^t + R() \times (x_{ij}^t - x_{kj}^t) & ; \quad f_i^t < f_k^t \\ x_{ij}^t + R() \times (x_{kj}^t - x_{ij}^t) & ; \quad \text{Otherwise} \quad (j = 1, 2, ..., S) \end{cases}. \tag{22}$$

3.8. Migration

It is observed that sometimes the algorithm attains premature convergence due to a decrease in the ability of learners to explore the search space. In order to increase the diversity of the learners, random individuals are introduced into each generation from the global search space. In order to increase the exploration of the search

space, *0.3NL* learners are randomly selected to start the migration operation. The jth subject score of the ith learner is randomly regenerated as:

$$x_{ij}^{t} = \begin{cases} G_j + R() \times (x_j^{\min} - G_j) & ; \quad \beta < \frac{(G_j - x_j^{\min})}{(x_j^{\max} - x_j^{\min})} \quad (j = 1, 2, ..., S) \\ G_j + R() \times (x_j^{\max} - G_j) & ; \quad \text{Otherwise} \end{cases}, \tag{23}$$

where G_j is the global best marks and R and β are uniform random numbers.

The selection of random individual x_{ij}^{t} is dependent on 2 uniform random numbers, R and β. The selection of a random individual near the lower limit or towards the upper limit of the variable range is determined by the value of β. Furthermore, the amount of variable value to be perturbed is decided by the value of R.

3.9. Best function values

Initially, at the end of the first iteration, the function value of the fittest learner is set as the global best (f^{best}), and corresponding marks scored by him in various subjects are set as global best marks (G_j). At the end of each iteration, if the function value obtained by the best learner is better than the global best (f^{best}), it then replaces the global best, and corresponding marks obtained by the best learner are stored as the global best marks (G_j).

3.10. Stopping criteria

A heuristic optimization algorithm can be stopped by employing various stopping criteria. Common examples are maximum number of iterations, tolerance, and number of function evaluations. ETLBO employs a maximum number of iterations as the criterion to stop. The above procedure is repeated with an incremented t value until the value of t reaches the maximum value of iterations specified. Otherwise, G_j is the best value of filter coefficients and f^{best} is the best/minimum value of the objective function.

3.11. Flowchart of ETLBO

The stepwise methodology of the ETLBO algorithm for the IIR filter design is presented in the form of a flowchart (Figure 3).

4. Design results and comparison

The validity of ETLBO for the design of IIR digital filters is established by comparing the obtained results with classical methods, TLBO, and techniques used by various researchers. The wide area of applicability of the proposed ETLBO method is demonstrated by designing digital IIR filters following different design criteria specified below:

- Minimum magnitude and phase response error while achieving the lowest filter order.
- Minimum magnitude and phase response error for higher orders of the digital IIR filter.

4.1. Minimum magnitude and phase response error while achieving the lowest filter order

The proposed ETLBO is successfully applied for the design of stable digital IIR HP, LP, BS, and BP filters by considering magnitude error and phase response while achieving the lowest order and stability constraints

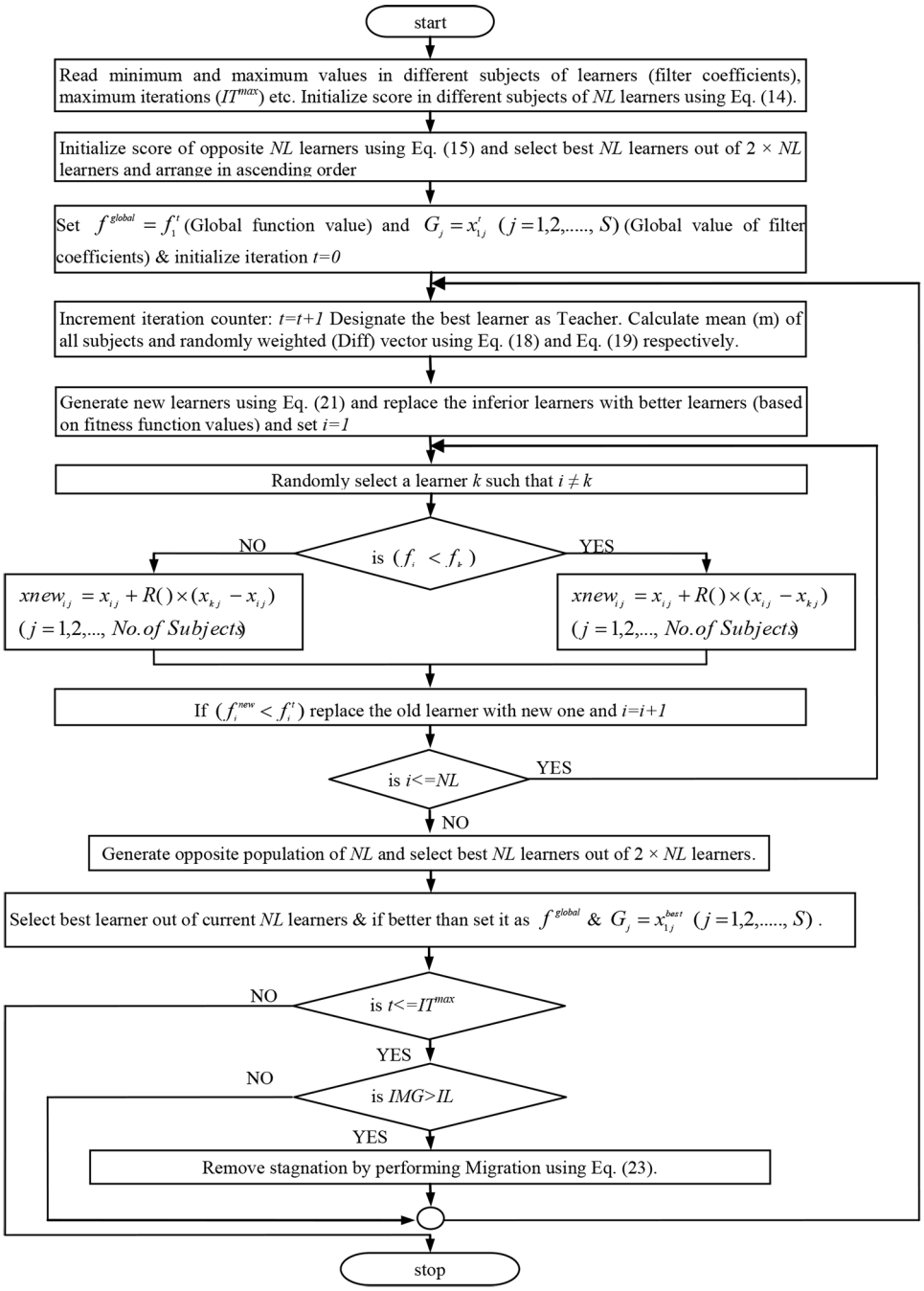

Figure 3. Flowchart of ETLBO.

Table 1. Prescribed design conditions for LP, HP, BP, and BS filters.

Filter type	Pass-band ($\delta_P = 0.1088$)	Stop-band ($\delta_s = 0.17783$)	Order
Low-pass (LP)	$0 \leq \omega \leq 0.2\pi$	$0.3\pi \leq \omega \leq \pi$	11
High-pass (HP)	$0.8\pi \leq \omega \leq \pi$	$0 \leq \omega \leq 0.7\pi$	11
Band-pass (BP)	$0.4\pi \leq \omega \leq 0.6\pi$	$0 \leq \omega \leq 0.25\pi$ $0.75 \leq \omega \leq \pi$	11
Band-stop (BS)	$0 \leq \omega \leq 0.25\pi$ $0.75 \leq \omega \leq \pi$	$0.4\pi \leq \omega \leq 0.6\pi$	11

stated by Eqs. (10a)–(10g). The design parameters followed for the design of IIR digital filters are presented in Table 1. For the design of the IIR digital filter, 200 evenly distributed points are chosen in the frequency span $[0, \pi]$. The order is selected as 11 as described in Section 2.4.

The examples of the IIR digital filters considered in [6,8,16] were used to test and compare the digital IIR filter designed with the proposed ETLBO algorithm. The designed LP, HP, BP, and BS digital IIR filters obtained employing the ETLBO approach representing the value of filter coefficients are shown in Eqs. (24)–(27):

$$H_{LP}(z) = 0.20462 \times \frac{(z + 0.258974)(z^2 - 0.95054z + 0.962161)}{(z - 0.39299)(z^2 - 1.21061z + 0.631761)}, \tag{24}$$

$$H_{HP}(z) = 0.222616 \times \frac{(z - 0.30596)(z^2 + 0.938134z + 0.945373)}{(z + 0.32509)(z^2 + 1.180231z + 0.613116)}, \tag{25}$$

$$H_{BP}(z) = 0.224529 \times \frac{(z^2 - 1.69079z + 1.066826)(z^2 + 1.678418z + 1.057463)}{(z^2 - 0.632174z + 0.511494)(z^2 - 0.63074z + 0.509961)}, \tag{26}$$

$$H_{BS}(z) = 0.467226 \times \frac{(z^2 + 0.279695z + 0.874784)(z^2 - 0.28008z + 0.871495)}{(z^2 + 0.746293z + 0.470755)(z^2 - 0.74687z + 0.471200)}. \tag{27}$$

The magnitude and phase response diagrams of HP, LP, BS, and BP digital IIR filters designed with the proposed ETLBO are presented in Figures 4 and 5.

The designed LP, HP, BP, and BS digital IIR filters with ETLBO were tested for stability by drawing pole-zero diagrams, shown in Figure 6. It is observed from Figure 6 that all the poles lie within the unit circle, which clearly signifies that the designed filters follow the stability constraints imposed in the design procedure.

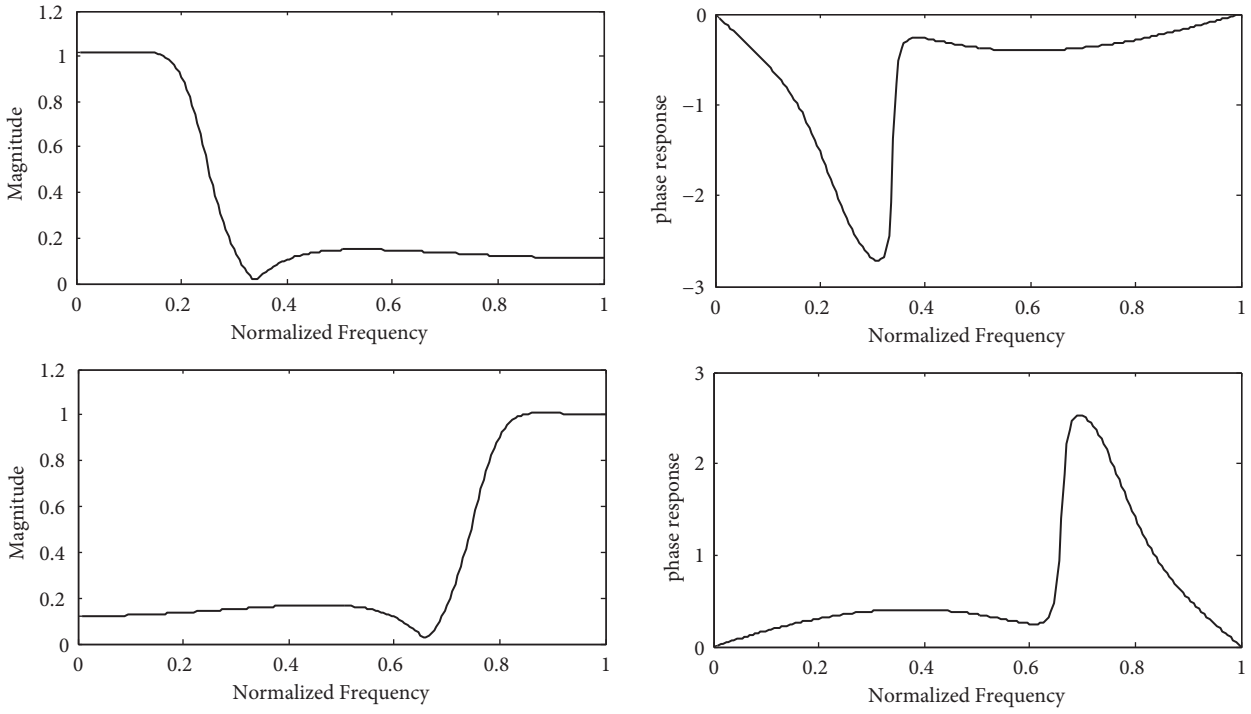

Figure 4. Magnitude and phase response of LP and HP filters.

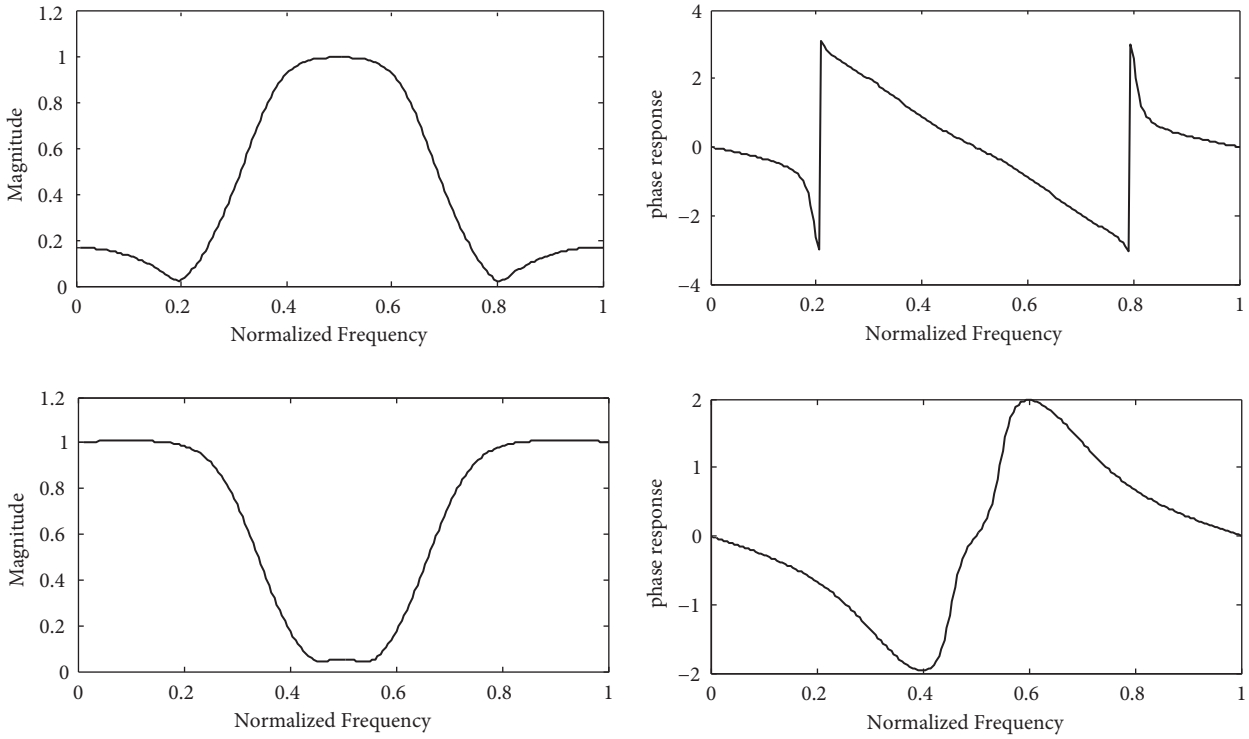

Figure 5. Magnitude and phase response of BP and BS filters.

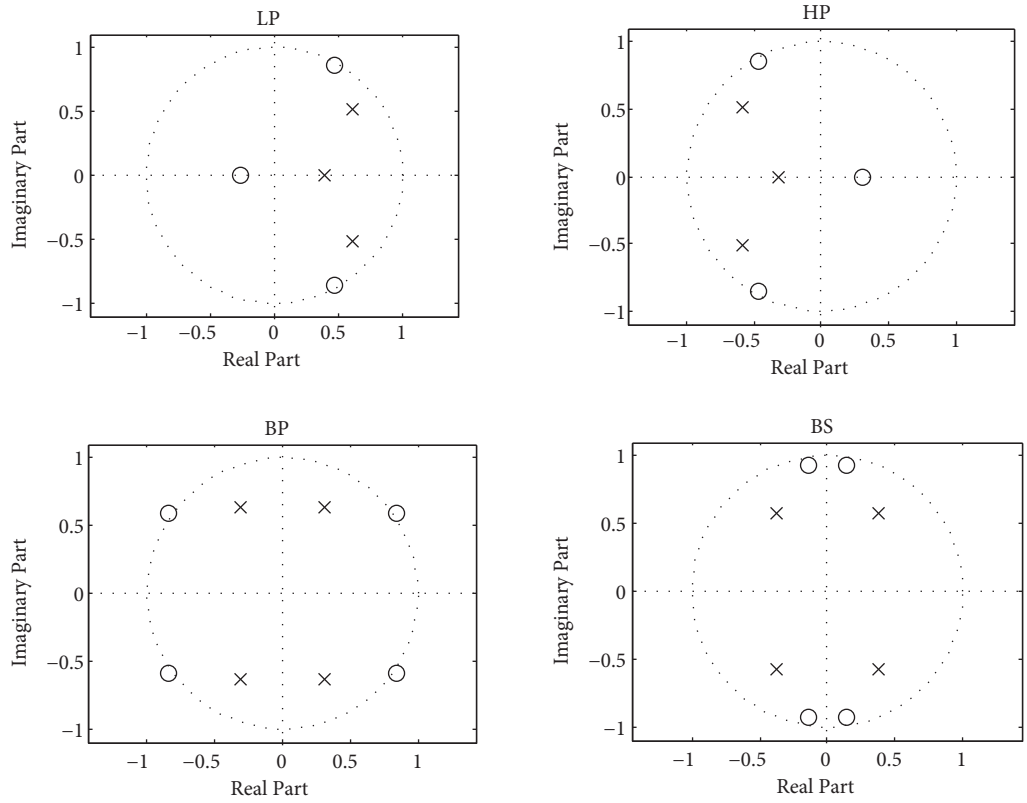

Figure 6. Pole-zero plots for LP, HP, BP, and BS filters, respectively.

The validity of the results obtained with the proposed ETLBO method has been established by comparing it with classical methods and other previously applied techniques.

- Comparison with classical methods: The data related to classical methods, namely Butterworth (BWTH), Chebyshev Type 1 (CHBY1), Chebyshev Type 2 (CHBY2), and Elliptic (ELTC) Function Considered for LS-MOEA [16], are referenced and a comparison is presented in Table 2. It can be observed from Table 2 that ETLBO and LS-MOEA provide the lowest orders in comparison to the classical methods.

Table 2. Comparison of lowest filter order with classical methods.

Filter	BWTH	CHBY1	CHBY2	ELTC	LS-MOEA	ETLBO
LP	6	4	4	3	3	3
HP	6	4	4	3	3	3
BP	12	8	8	6	4	4
BS	12	8	8	6	4	4

- Comparison with previously applied techniques: The comparison of ETLBO is done with TLBO, HGA [6], CCGA [8], and LS-MOEA [16] in terms of function evaluation size, lowest filter order, magnitude performance in pass-band and stop-band, phase response error, and ripples in pass-band and stop-band. The compiled results are shown in Table 3. From the evaluated results in Table 3, it is concluded that the proposed ETLBO algorithm enhances the performance of TLBO. The performance of the proposed ETLBO approach in comparison to HGA [6], CCGA [8], and LS-MOEA [16] is as given below:

- In comparison to [6], [8], and [16], the proposed ETLBO approach gives the best results in terms of pass-band and stop-band magnitude performance for the LP digital IIR filter.

- The HP digital IIR filter designed with the ETLBO approach gives a lower number of ripples in the stop-band in comparison to [6], [8], and [16].

- The performance of the designed BP digital IIR filter with the ETLBO approach is best and surpasses [6], [8], and [16] in terms of ripples in the pass-band. Ripples obtained with ETLBO in the stop-band are fewer in comparison to [6] and [16], and comparable with [8].

- For the designed BS filter with ETLBO, pass-band magnitude performance is better in comparison to [8] and [16], and comparable with [6]. The stop-band magnitude performance of the designed BS filter with ETLBO is best in comparison to [6], [8], and [16].

- Phase response error of the designed HP, LP, BS, and BP filters with the ETLBO approach is lowest and best in comparison to [6], [8], and [16].

- In terms of lowest order, ETLBO, LS-MOEA, and CCGA are equivalent and are better than HGA.

- The number of function evaluations of ETLBO are minimum in the case of the BS filter and second-best in the cases of HP, LP, and BP filters. The marginally higher computational cost in the cases of HP, LP, and BP filters incurred by employing ETLBO is compensated for by better obtained results. The number of the function evaluation (FES) of ETLBO is calculated as follows:

Table 3. Comparison of design results for LP, HP, BP, and BS filters.

	Fitness evaluation size	Lowest filter order	Pass-band magnitude performance (ripple magnitude)	Stop-band magnitude performance (ripple magnitude)	Phase response error
LP filter					
HGA [6]	-	3	$0.8862 \leq \lvert H(e^{jw})\rvert \leq 1.0$ (0.1138)	$\lvert H(e^{jw})\rvert \leq 0.1800$ (0.1800)	1.6485×10^{-4}
CCGA [8]	1.4248×10^{5}	3	$0.9034 \leq \lvert H(e^{jw})\rvert \leq 1.0$ (0.0966)	$\lvert H(e^{jw})\rvert \leq 0.1669$ (0.1669)	1.4749×10^{-4}
LS-MOEA [16]	4.9×10^{3}	3	$0.9083 \leq \lvert H(e^{jw})\rvert \leq 1.0$ (0.0917)	$\lvert H(e^{jw})\rvert \leq 0.1586$ (0.1586)	1.0959×10^{-4}
TLBO	6.01×10^{4}	3	$0.9096 \leq \lvert H(e^{jw})\rvert \leq 1.0$ (0.0904)	$\lvert H(e^{jw})\rvert \leq 0.1507$ (0.1507)	1.0706×10^{-4}
ETLBO	4.52×10^{4}	3	$0.9099 \leq \lvert H(e^{jw})\rvert \leq 1.0$ (0.0901)	$\lvert H(e^{jw})\rvert \leq 0.1514$ (0.1514)	1.06712×10^{-4}
HP filter					
HGA [6]	-	3	$0.9221 \leq \lvert H(e^{jw})\rvert \leq 1.0$ (0.0779)	$\lvert H(e^{jw})\rvert \leq 0.1819$ (0.1819)	1.1212×10^{-4}
CCGA [8]	3.4164×10^{5}	3	$0.9044 \leq \lvert H(e^{jw})\rvert \leq 1.0$ (0.0956)	$\lvert H(e^{jw})\rvert \leq 0.1749$ (0.1749)	9.7746×10^{-4}
LS-MOEA [16]	4.2385×10^{4}	3	$0.9004 \leq \lvert H(e^{jw})\rvert \leq 1.0$ (0.0996)	$\lvert H(e^{jw})\rvert \leq 0.1746$ (0.1746)	9.6150×10^{-5}
TLBO	7.01×10^{4}	3	$0.9004 \leq \lvert H(e^{jw})\rvert \leq 1.0$ (0.0996)	$\lvert H(e^{jw})\rvert \leq 0.1745$ (0.1745)	9.4708×10^{-5}
ETLBO	6.02×10^{4}	3	$0.9043 \leq \lvert H(e^{jw})\rvert \leq 1.0$ (0.0957)	$\lvert H(e^{jw})\rvert \leq 0.1700$ (0.1700)	9.4327×10^{-5}
BP filter					
HGA [6]	-	6	$0.8956 \leq \lvert H(e^{jw})\rvert \leq 1.0$ (0.1044)	$\lvert H(e^{jw})\rvert \leq 0.1772$ (0.1772)	1.1222×10^{-4}
CCGA [8]	7.7896×10^{5}	4	$0.8920 \leq \lvert H(e^{jw})\rvert \leq 1.0$ (0.1080)	$\lvert H(e^{jw})\rvert \leq 0.1654$ (0.1654)	8.1751×10^{-5}
LS-MOEA [16]	9.995×10^{3}	4	$0.9285 \leq \lvert H(e^{jw})\rvert \leq 1.0$ (0.0715)	$\lvert H(e^{jw})\rvert \leq 0.1734$ (0.1734)	6.0371×10^{-5}
TLBO	5.01×10^{4}	4	$0.9286 \leq \lvert H(e^{jw})\rvert \leq 1.0$ (0.0714)	$\lvert H(e^{jw})\rvert \leq 0.1704$ (0.1704)	4.8980×10^{-5}
ETLBO	4.22×10^{4}	4	$0.9290 \leq \lvert H(e^{jw})\rvert \leq 1.0$ (0.0710)	$\lvert H(e^{jw})\rvert \leq 0.1701$ (0.1701)	4.5162×10^{-5}
BS filter					
HGA [6]	-	4	$0.8920 \leq \lvert H(e^{jw})\rvert \leq 1.0$ (0.1080)	$\lvert H(e^{jw})\rvert \leq 0.1726$ (0.1726)	2.7074×10^{-4}
CCGA [8]	7.7532×10^{5}	4	$0.8966 \leq \lvert H(e^{jw})\rvert \leq 1.0$ (0.1034)	$\lvert H(e^{jw})\rvert \leq 0.1733$ (0.1733)	1.6119×10^{-4}
LS-MOEA [16]	1.23505×10^{5}	4	$0.8967 \leq \lvert H(e^{jw})\rvert \leq 1.0$ (0.1033)	$\lvert H(e^{jw})\rvert \leq 0.1725$ (0.1725)	1.5084×10^{-4}
TLBO	7.01×10^{4}	4	$0.8937 \leq \lvert H(e^{jw})\rvert \leq 1.0$ (0.1063)	$\lvert H(e^{jw})\rvert \leq 0.1721$ (0.1721)	1.5011×10^{-4}
ETLBO	6.62×10^{4}	4	$0.8945 \leq \lvert H(e^{jw})\rvert \leq 1.0$ (0.1055)	$\lvert H(e^{jw})\rvert \leq 0.1724$ (0.1724)	1.4586×10^{-4}

$$FES_{ETLBO} = 2 \times NL + ((3 \times NL) \times IT^{\max}), \tag{28}$$

where NL is the number of learners and IT^{max} is the maximum number of iterations.

Moreover, the results of the trend of magnitude response error versus phase response error depicted in Figure 7 clearly justify the Pareto optimal front.

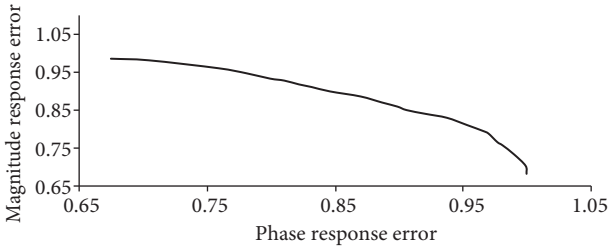

Figure 7. Variation of magnitude response error vs. phase response error applying ETLBO.

4.2. Minimum magnitude and phase response error for higher orders of the digital IIR filter

The versatility of the proposed ETLBO method for the design of IIR digital filters is further established by approximating the digital IIR filter in terms of magnitude and phase response simultaneously for higher orders of the filter by varying u and v in the first and second-order blocks, respectively. The magnitude response errors in terms of ripples in the pass-band, stop-band, and phase response error obtained for HP, LP, BS, and BP filters with ETLBO by varying first- and second-order blocks are summarized in Tables 4–6.

Table 4. Design results for higher-order LP digital IIR filter applying ETLBO.

Order	Minimum magnitude in pass-band (maximum magnitude = 1)	Stop-band ripples	Phase response error	Order	Minimum magnitude in pass-band (maximum magnitude = 1)	Stop-band ripples	Phase response error
3	0.90999	0.15148	1.0×10^{-4}	17	0.93226	0.14900	2.80×10^{-5}
4	0.91358	0.14000	1.1×10^{-4}	18	0.91089	0.13782	1.34×10^{-5}
5	0.91711	0.13990	9.51×10^{-5}	19	0.93941	0.12480	6.11×10^{-5}
6	0.91427	0.13739	9.63×10^{-5}	20	0.93751	0.13780	4.77×10^{-5}
7	0.91662	0.14125	8.91×10^{-5}	21	0.91392	0.11246	6.09×10^{-5}
8	0.91493	0.13948	9.16×10^{-5}	22	0.92178	0.12192	5.11×10^{-5}
9	0.92504	0.12074	3.81×10^{-5}	23	0.92950	0.13509	8.16×10^{-5}
10	0.91527	0.13672	9.58×10^{-5}	24	0.90917	0.14295	7.57×10^{-5}
11	0.92458	0.12867	8.83×10^{-5}	25	0.90836	0.11680	9.48×10^{-4}
12	0.92206	0.13488	9.88×10^{-5}	26	0.89615	0.11816	7.53×10^{-5}
13	0.91267	0.14311	1.75×10^{-5}	27	0.93521	0.16698	9.09×10^{-5}
14	0.91026	0.12245	3.08×10^{-5}	28	0.91873	0.13305	3.80×10^{-5}
15	0.92032	0.14853	1.73×10^{-5}	29	0.91130	0.14223	6.59×10^{-5}
16	0.91738	0.14625	2.68×10^{-5}	30	0.91273	0.14684	8.37×10^{-5}

The results depicted in Tables 4–6 clearly demonstrate the consistency of the proposed ETLBO algorithm for the design of digital IIR filters of higher orders. The best results in terms of magnitude and phase response for digital IIR filters obtained with ETLBO by varying first- and second-order blocks are shown in Table 7.

The results obtained for best stable digital IIR filters obtained using ETLBO, presented in Table 7, undoubtedly validate that the best stable digital IIR filter results obtained using ETLBO outperform the results obtained by [6,8,16] depicted in Table 3. Although the order of the filter obtained is higher, it can be used for applications like image processing, communication systems, and audio processing, where linear phase response is highly required.

Table 5. Design results for higher order HP digital IIR filter applying ETLBO.

Order	Minimum magnitude in pass-band (maximum magnitude = 1)	Stop-band ripples	Phase response error	Order	Minimum magnitude in pass-band (maximum magnitude = 1)	Stop-band ripples	Phase response error
3	0.90430	0.17006	9.43×10^{-5}	17	0.93464	0.16390	1.90×10^{-4}
4	0.90383	0.16981	9.42×10^{-5}	18	0.91537	0.14869	1.11×10^{-4}
5	0.90971	0.16843	8.40×10^{-5}	19	0.92657	0.16274	1.14×10^{-4}
6	0.90456	0.16995	5.70×10^{-5}	20	0.91155	0.16941	9.94×10^{-5}
7	0.91142	0.16701	7.68×10^{-5}	21	0.91113	0.18114	9.93×10^{-5}
8	0.90563	0.16857	7.45×10^{-5}	22	0.90650	0.17088	1.71×10^{-4}
9	0.91136	0.16716	8.63×10^{-5}	23	0.91311	0.16531	1.70×10^{-4}
10	0.92108	0.16992	9.45×10^{-5}	24	0.95563	0.17152	2.02×10^{-4}
11	0.90468	0.16926	7.10×10^{-5}	25	0.92498	0.15432	2.35×10^{-4}
12	0.90668	0.16608	7.84×10^{-5}	26	0.88311	0.20022	2.06×10^{-4}
13	0.90939	0.16169	7.81×10^{-5}	27	0.61058	0.19365	5.89×10^{-4}
14	0.90403	0.16123	1.00×10^{-4}	28	0.85029	0.21569	1.16×10^{-4}
15	0.91051	0.16871	9.35×10^{-5}	29	0.79982	0.18429	8.26×10^{-4}
16	0.93452	0.16682	1.51×10^{-4}	30	0.87075	0.25893	5.95×10^{-5}

Table 6. Design results for higher-order BP and BS digital IIR filter applying ETLBO.

BP filter				BS filter			
Order	Minimum magnitude in pass-band (maximum magnitude = 1)	Stop-band ripples	Phase response error	Order	Minimum magnitude in pass-band (maximum magnitude = 1)	Stop-band ripples	Phase response error
4	0.92904	0.17018	4.51×10^{-5}	4	0.89455	0.17244	1.45×10^{-4}
6	0.92670	0.14134	4.84×10^{-4}	6	0.89373	0.16322	2.03×10^{-4}
8	0.92037	0.19160	2.72×10^{-5}	8	0.89873	0.15281	2.55×10^{-4}
10	0.92063	0.16150	9.61×10^{-4}	10	0.89397	0.11156	4.52×10^{-4}
12	0.92170	0.17581	3.86×10^{-4}	12	0.89899	0.17234	2.40×10^{-4}
14	0.96624	0.17988	5.96×10^{-4}	14	0.90739	0.17243	1.40×10^{-4}
16	0.92423	0.16128	3.10×10^{-3}	16	0.87001	0.18528	7.13×10^{-5}
18	0.92776	0.16022	6.02×10^{-4}	18	0.89868	0.17150	2.46×10^{-4}
20	0.92573	0.19435	1.79×10^{-5}	20	0.88411	0.18440	6.90×10^{-5}
22	0.91556	0.20551	2.63×10^{-5}	22	0.89302	0.17143	2.54×10^{-4}
24	0.91619	0.19553	4.24×10^{-5}	24	0.88213	0.16006	2.04×10^{-4}
26	0.92418	0.21103	3.60×10^{-5}	26	0.87979	0.18627	9.72×10^{-5}
28	0.91382	0.19642	5.74×10^{-5}	28	0.93227	0.10409	7.76×10^{-4}
30	0.91131	0.21907	4.74×10^{-5}	30	0.86324	0.19154	7.77×10^{-5}

Furthermore, the robustness of ETLBO was validated by performing 100 independent runs. The minimum, maximum, average, and standard deviation values of the fitness function obtained are summarized in Table 8, which clearly depicts that ETLBO is a robust algorithm with a small value of standard deviation. The trend of the fitness function obtained with ETLBO with respect to iterations for all types of IIR digital filters shown in Figure 8 clearly emphasizes that ETLBO attains a global solution in a fixed number of iterations. Furthermore, the trend obtained for the fitness function by varying the number of learners/population

presented in Figure 9 establishes that ETLBO is insensitive to its only controlling parameter, i.e. the number of learners/population. The increase in learners gives better fitness at the cost of function evaluations.

Table 7. Best performance of IIR filter designed with ETLBO.

Filter type	Magnitude response in pass-band	Magnitude response in stop-band	Phase response error	Lowest order
LP	$0.9250 \leq \lvert H(e^{jw}) \rvert \leq 1.0$	$\lvert H(e^{jw}) \rvert \leq 0.1207$	3.8174×10^{-5}	9
HP	$0.9045 \leq \lvert H(e^{jw}) \rvert \leq 1.0$	$\lvert H(e^{jw}) \rvert \leq 0.1699$	5.7010×10^{-5}	6
BP	$0.9203 \leq \lvert H(e^{jw}) \rvert \leq 1.0$	$\lvert H(e^{jw}) \rvert \leq 0.1916$	2.7223×10^{-5}	8
BS	$0.9073 \leq \lvert H(e^{jw}) \rvert \leq 1.0$	$\lvert H(e^{jw}) \rvert \leq 0.1724$	1.4013×10^{-4}	14

Table 8. Variation of fitness function for IIR filter designed with ETLBO*.

Type of filter	Minimum	Maximum	Average	Standard deviation
LP	0.9998547	0.9999981	0.999922895	4.28697×10^{-5}
HP	0.9998368	0.9999880	0.99988083	4.0086×10^{-5}
BP	0.9999879	0.9996773	0.999869104	5.25238×10^{-5}
BS	0.9997436	0.99997749	0.99987791	4.4558×10^{-5}
*The values have been recorded with 100 random runs.				

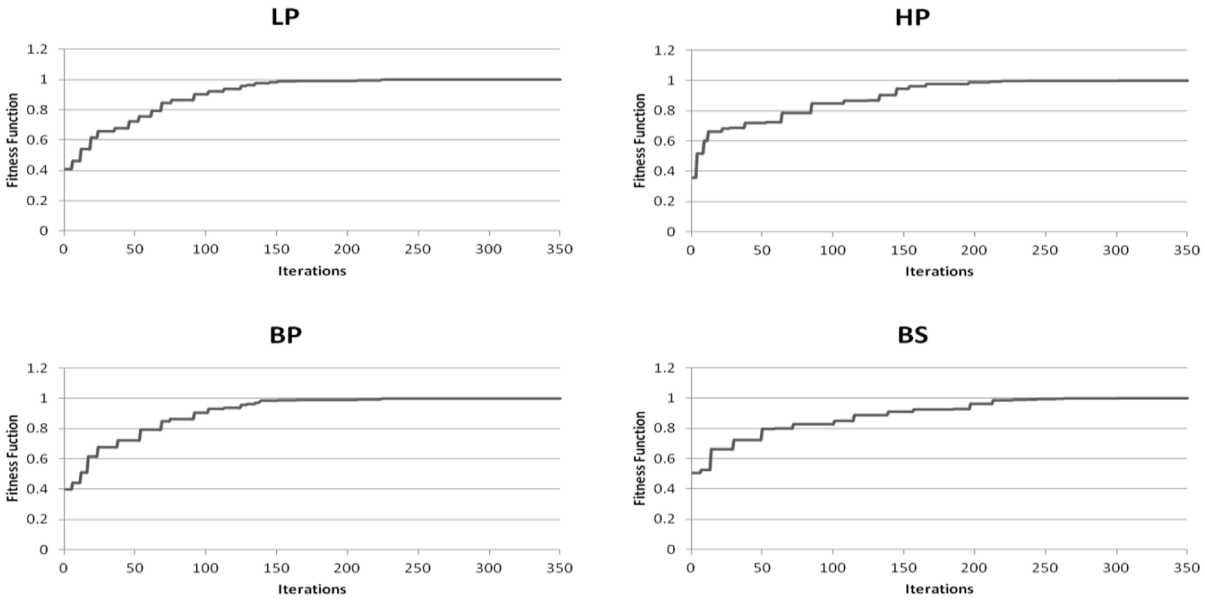

Figure 8. Variation of fitness function with iterations for designed digital IIR filter applying ETLBO.

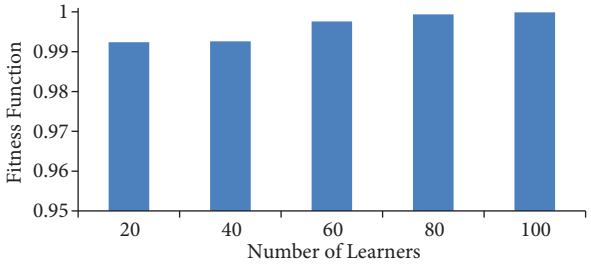

Figure 9. Variation of fitness function with learners/population for designed digital IIR filter applying ETLBO.

5. Conclusion

In this paper, the ETLBO algorithm is successfully implemented to design the LP, HP, BP, and BS digital IIR filters in a multiobjective framework. A fuzzy set theory approach has been exploited to establish the best compromise solution involving a multiplicity of objectives. The performance of ETLBO is enhanced by initializing the population by applying opposition-based learning. Furthermore, migration has been applied to maintain the diversity and search space exploration, and avoid premature convergence. The effectiveness of the proposed ETLBO has been also examined for the higher-order filter, and robustness was verified through 100 independent runs. The comparisons of the obtained results reveal the efficiency of the developed ETLBO approach over other existing methods for digital IIR filter design. The results show that the proposed ETLBO approach is efficient and generates multiple Pareto-optimal solutions in a single run. The ETLBO algorithm is effectively applied to design digital IIR filters of all types and has given considerable improvement in terms of results and convergence.

References

[1] Antoniou A. Digital Signal Processing: Signals, Systems and Filters. New York, NY, USA: McGraw-Hill, 2005.

[2] Boudjelaba K, Ros F, Chikouche D. An efficient hybrid genetic algorithm to design finite impulse response filters. Expert Syst Appl 2014; 41: 5917-5937.

[3] Lu WS, Antoniou A. Design of digital filters and filter banks by optimization: a state of the art review. In: Signal Processing X: Theories and Applications. Proceedings of EUSIPCO 2000, Tenth European Signal Processing Conference; 4–8 September 2000; Tampere, Finland. Tampere: TTKK-Paino. pp. 351-354.

[4] Lang MC. Algorithms for the constrained design of digital filters with arbitrary magnitude and phase responses. PhD, Vienna University of Technology, Vienna, Austria, 1999.

[5] Proakis JG, Manolakis DG. Digital Signal Processing: Principles, Algorithms, and Applications. New Delhi, India: Pearson Education, 2007.

[6] Tang KS, Man KF, Kwong S, Liu ZF. Design and optimization of IIR filter structure using hierarchical genetic algorithms. IEEE T Ind Elecron 1998; 45: 481-487.

[7] Tsai JT, Chou JH, Liu TK. Optimal design of digital IIR filters by using hybrid Taguchi genetic algorithm. IEEE T Ind Electron 2006; 53: 867-879.

[8] Yu Y, Xinjie Y. Cooperative coevolutionary genetic algorithm for digital IIR filter design. IEEE T Ind Electron 2007; 54: 1311-1318.

[9] Chen S, Istepanian RH, Luk BL. Digital IIR filter design using adaptive simulated annealing. Digit Signal Process 2001; 11: 241-251.

[10] Karaboga N, Kalinli A, Karaboga D. Designing IIR filters using ant colony optimisation algorithm. Eng Appl Artif Intell 2004; 17: 301-309.

[11] Kalinli A, Karaboga N. A new method for adaptive IIR filter design based on Tabu search algorithm. J Electron Commun 2005; 59: 111-117.

[12] Tsai JT, Chou JH. Optimal design of digital IIR filters by using an improved immune algorithm. IEEE T Signal Proces 2006; 54: 4582-4596.

[13] Chen S, Luk BL. Digital IIR filter design using particle swarm optimisation. Int J Model Ident Control 2010; 9: 327-335.

[14] Dai C, Chen W, Zhu Y. Seeker optimization algorithm for digital IIR filter design. IEEE T Ind Electron 2010; 57: 1710-1718.

[15] Tsai CW, Huang CH, Lin CL. Structure-specified IIR filter and control design using real structured genetic algorithm. Appl Soft Comput 2010; 9: 1285-1295.

[16] Wang Y, Li B, Chen Y. Digital IIR filter design using multi-objective optimization evolutionary algorithm. Appl Soft Comput 2011; 11: 1851-1857.

[17] Li B, Wang Y, Weise T, Long L. Fixed-point digital IIR filter design using two-stage ensemble evolutionary algorithm. Appl Soft Comput 2013; 13: 329-338.

[18] Saha SK, Kar R, Mandal D, Ghoshal SP. Gravitation search algorithm: application to the optimal IIR filter design. J King Saud Univ Eng Sci 2014; 26: 69-81.

[19] Rao RV, Savsani VJ, Vakharia DP. Teaching-learning-based optimization: a novel method for constrained mechanical design optimization problems. Comput Aided D 2011; 43: 303-315.

[20] Rao RV, Savsani VJ, Vakharia DP. Teaching-learning-based optimization: a novel optimization method for continuous non-linear large scale problems. Inform Sciences 2012; 183: 1-15.

[21] Rao R, Patel V. An elitist teaching-learning-based optimization algorithm for solving complex constrained optimization problems. Int J Ind Eng Comput 2012; 3: 535-560.

[22] Niimura T, Nakashima T. Multiobjective tradeoff analysis of deregulated electricity transactions. Int J Electr Pow Energ Syst 2003; 25: 179-185.

[23] Deczky AG. Synthesis of recursive filters using the minimum p-error criterion. IEEE T Acoust Speech 1972; 20: 257-263.

[24] Jury I. Theory and Application of the Z-Transform Method. New York, NY, USA: Wiley, 1964.

[25] Tapia CG, Murtagh BA. Interactive fuzzy programming with preference criteria in multiobjective decision-making. Comput Operat Res 1991; 18: 307-316.

[26] Roy PK. Teaching learning based optimization for short-term hydrothermal scheduling problem considering valve point effect and prohibited discharge constraint. Int J Electr Pow Energ Syst 2013; 53: 10-19.

[27] Tizhoosh H. Opposition-based learning: a new scheme for machine intelligence. In: International Conference on Computational Intelligence for Modelling, Control, and Automation 2005; 28–30 November 2005; Vienna, Austria. Los Alamitos, CA, USA: IEEE Computer Society. pp. 695-701.

[28] Rahnamayan S, Tizhoosh H, Salama MMA. Opposition-based differential evolution. IEEE T Evol Comput 2008; 12: 64-78.

[29] Singh M, Panigrahi BK, Abhyankar AR. Optimal coordination of directional over-current relays using teaching learning-based optimization (TLBO) algorithm. Int J Elec Power 2013; 50: 33-41.